Supporting Information

Tuning Electrochemical Properties of Tungsten Oxides Nanoplates via Sn Doping and Mixed-Phase Formation for Superior Quasi-Solid-State Supercapacitor

Harishchandra S. Nishad,[a] Rajesh R. Jaiswar,[a] Diwakar Singh,[b] Shekhar Bhame,[c] Shashikant P. Patole,[d] Pravin S. Walke[*a]

[a]National Centre for Nanosciences and Nanotechnology, University of Mumbai, Mumbai- India- 400098.
[b]Department of Metallurgical Engineering and Material Science, Indian Institute of Technology, IIT Bombay.
[c]Symbiosis Institute of Technology, Symbiosis International (Deemed University), Pune 412115, India
[d]Department of Physics, Khalifa University of Science and Technology, Abu Dhabi- 127788, UAE.

1. Electrochemical measurement

The electrochemical property of W0, SnW5, SnW10, SnW200, SnW400 and SnW600 was studied by PGSTAT302N Autolab system with a three-electrode setup. The glassy carbon electrode, platinum wire electrode, and Ag/AgCl serving as the working, counter, and reference electrodes, respectively. However, the specific capacitance, energy density, and power density was obtained by utilizing the below equations respectively.

1.1 Specific Capacitance from CV curve,

$$C_S = \frac{1}{2.m.v.\Delta V} \int_{Vmin}^{Vmax} I(V)dv \quad (\text{F g}^{-1}) \qquad \text{......... (S1)}$$

Here, C_s denotes the specific capacitance, m is the mass of the active material, v represents the scan rate, V_{max} and V_{min} indicate the operating potential window of the CV curve, I is the current, and ΔV is the potential.

1.2 Specific Capacitance from GCD curve,

$$C_s = \frac{I \ X \ \Delta t}{m \ X \ \Delta V} \quad (\text{F g}^{-1}) \qquad \text{.......... (S2)}$$

where, I - Current (A), m - Mass loading on electrode, Δt - Discharge time (s), ΔV^- Potential Window (V),

1.3 Energy density,

$$Eg = \frac{Cs \ X \ V^2}{2} \quad \text{(W h kg}^{-1})\qquad\qquad\qquad \text{.......... (S3)}$$

Where, Cs-Specific Capacitance (F g^{-1}), V-Potential Window (V), and

1.4 Power Density,

$$P = \frac{Eg}{\Delta t} \quad \text{(W kg}^{-1})\qquad\qquad\qquad \text{.......... (S4)}$$

Where, Eg - Energy Density (W h kg^{-1}), Δt - Discharge time.

2. Gel-electrolyte preparation

The gel electrolyte was prepared by adding 2 g of PVA in 20 mL of under constant heating and stirring at 70 ºC until a clear homogeneous solution was obtained. Then, an appropriate amount of H_2SO_4 was drop-wise added into the mixture. Further, the obtained solution was stirred till cool at room temperature naturally.

3. Mass balancing

The mass balancing of quasi-solid state asymmetric supercapacitor fabrication (QSSAS) was done with equation number 4. However, SnW200 used as a negative electrode and activated carbon (AC) used as positive electrode. The specific capacitance SnW200 is 167 F g-1 at 10 mV s^{-1} and the specific capacitance of AC is 116 F g^{-1} at 10 mV s^{-1}.

$$\frac{M^+}{M^-} = \frac{Cs^-}{Cs^+} \ x \ \frac{\Delta V^-}{\Delta V^+}\qquad\qquad\qquad \text{.......... (S5)}$$

where, the Cs^+; Cs^- and ΔV^+; ΔV^- represents capacitance value and potential window of anode and cathode respectively. The positive electrode was loaded with 1.5 mg of AC (M^+), the negative electrode was loaded with 2 mg (M^-) of SnW200.

4. Quasi-solid state asymmetric supercapacitor (QSSAS) fabrication

In the QSSAS device, Whatman-42 filter paper (as a separator) soaked in the gel electrolyte for the proper electrolyte filling. The anode was prepared by dispersing 5 mg

of activated carbon (AC) and 5 μL of Nafion binder in 0.5 mL of deionized (DI) water, followed by sonication for 3 minutes to obtain a well-dispersed mixture. From this mixture, 0.15 mL was drop-cast onto a carbon paper and dried under an IR lamp for 10 minutes. Similarly, 0.2 mL of the corresponding mixture SnW200 was drop-cast onto a carbon paper for the negative electrode and dried under identical conditions. Thus 1.5 mg mass was loaded on anode electrode and 2 mg on cathode electrode was packed in a
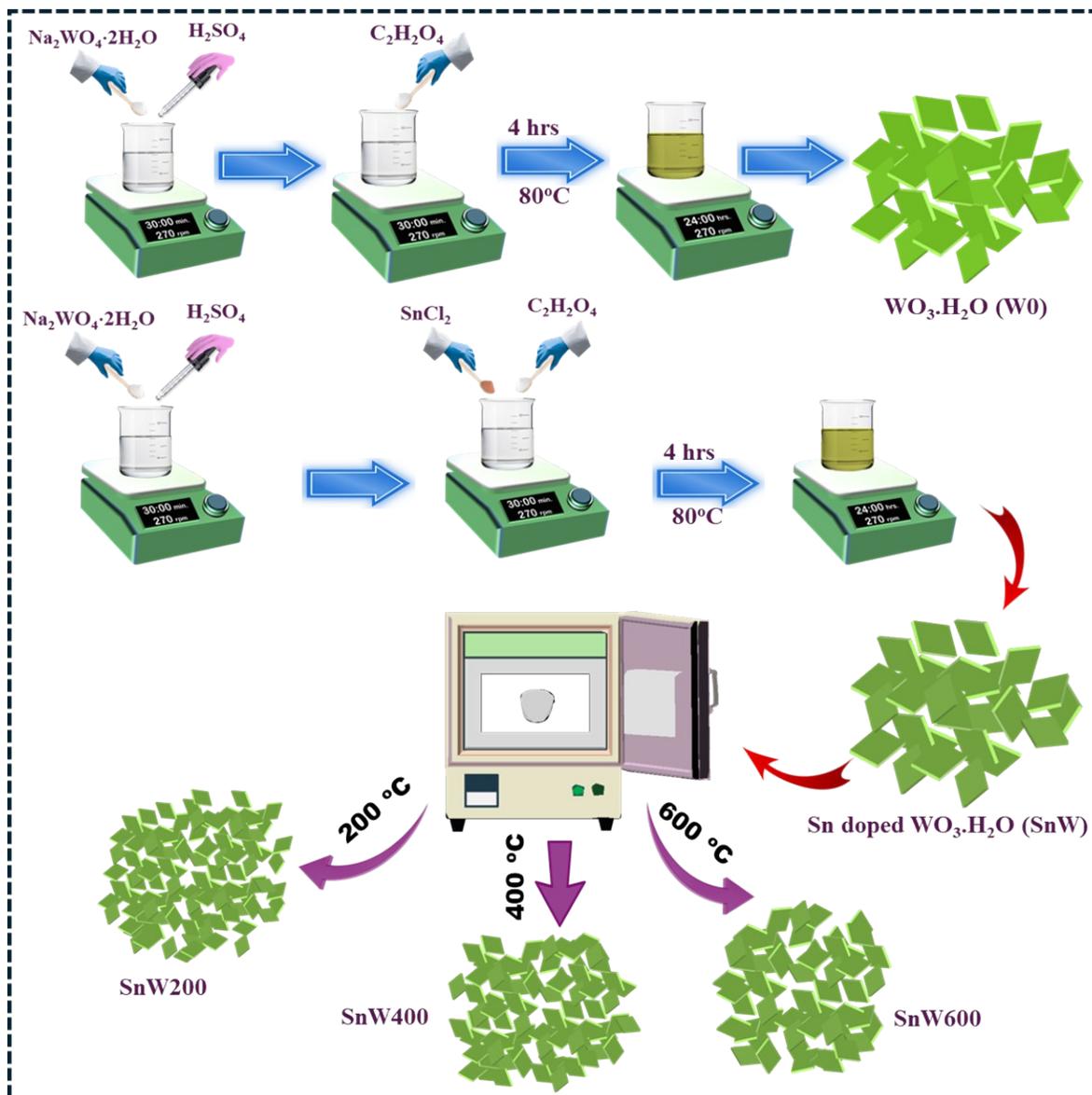

Fig. S1 Schematic sketch of W0, SnW5, and SnW00, SnW400, and SnW600 preparation setup.

Swagelok cell with the separator and gel electrolyte. The formulae used for mass balancing is given in the Supplementary information.
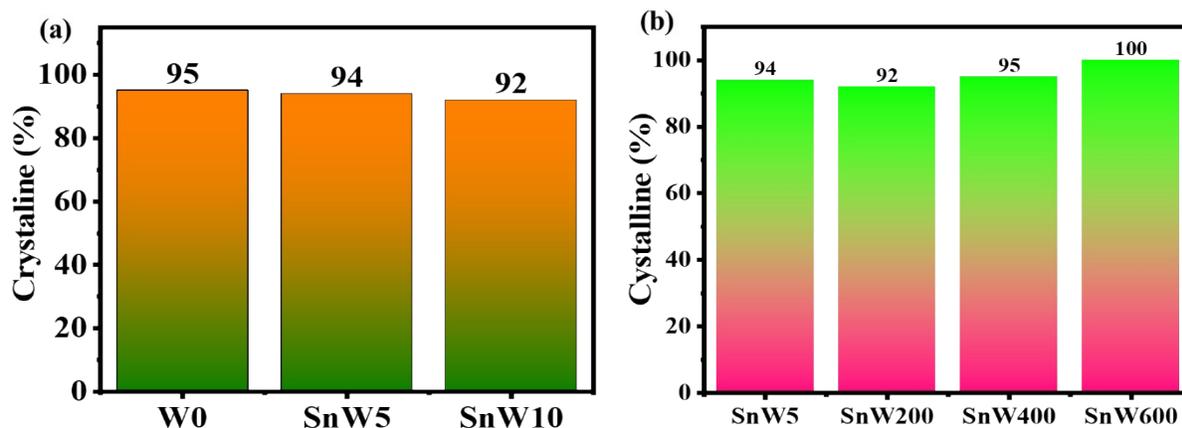
Fig. S2 Bar graph of crystallinity of W0, SnW5, SnW10 (a), and SnW5, SnW200, SnW400, and SnW600 (b).
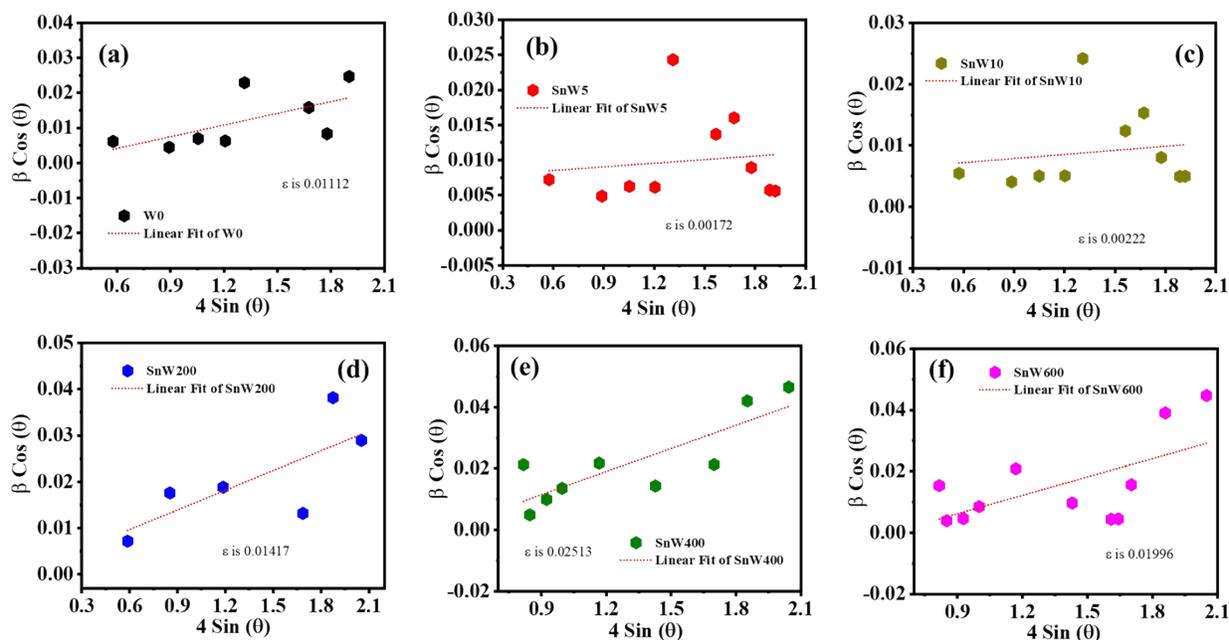

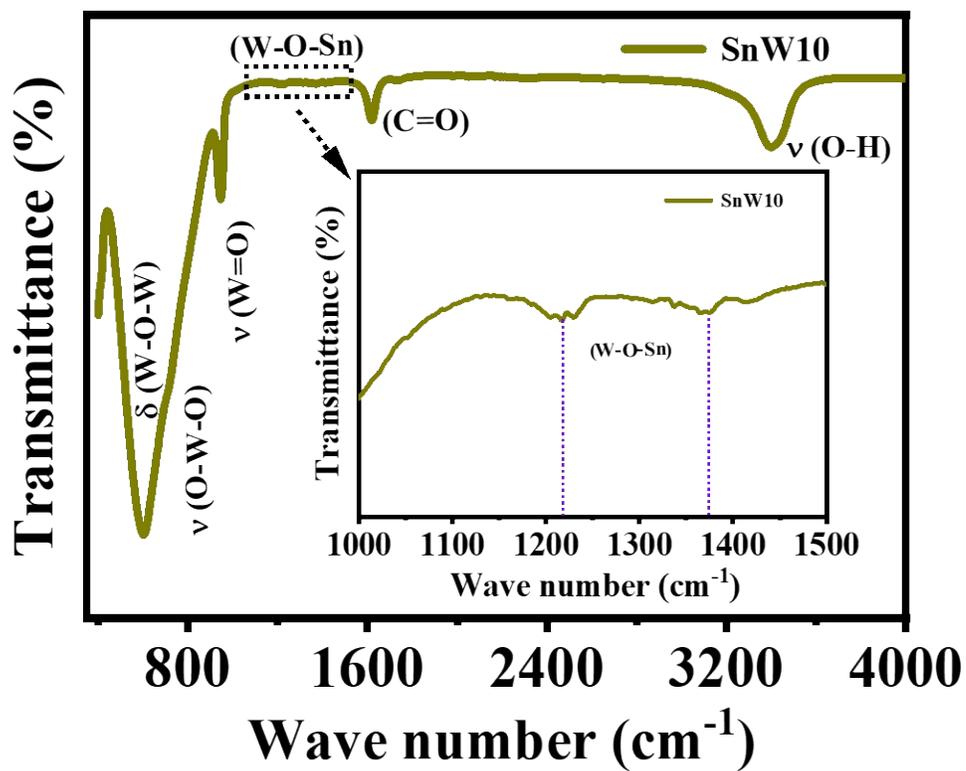Fig. S3 (a-c) W-H plot of W0, SnW5, SnW10, (d-f) W-H plot of SnW200, SnW400, and SnW600.

4

Fig. S4 FT-IR spectra of SnW10 and inset is magnified FT-IR spectra of selected region of Fig. 3(b).
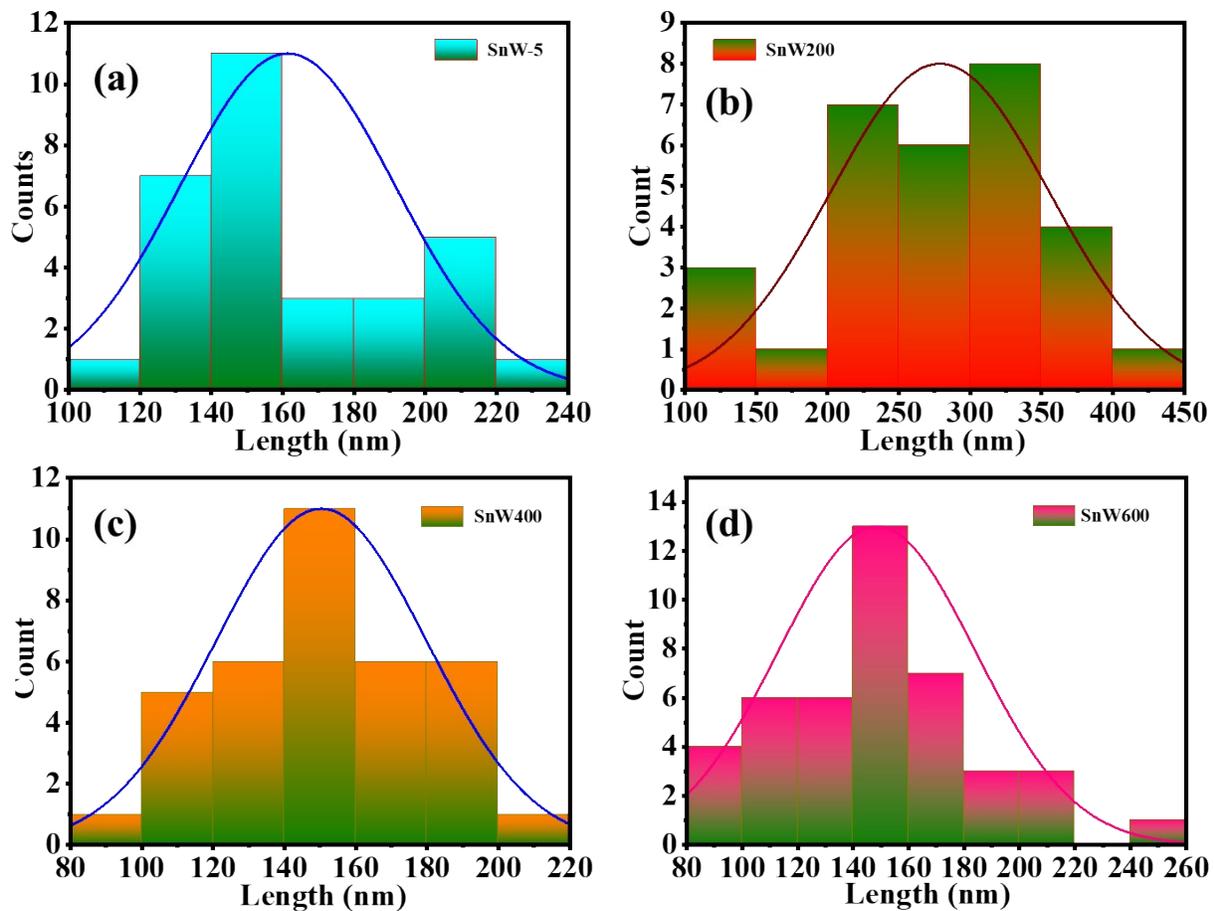
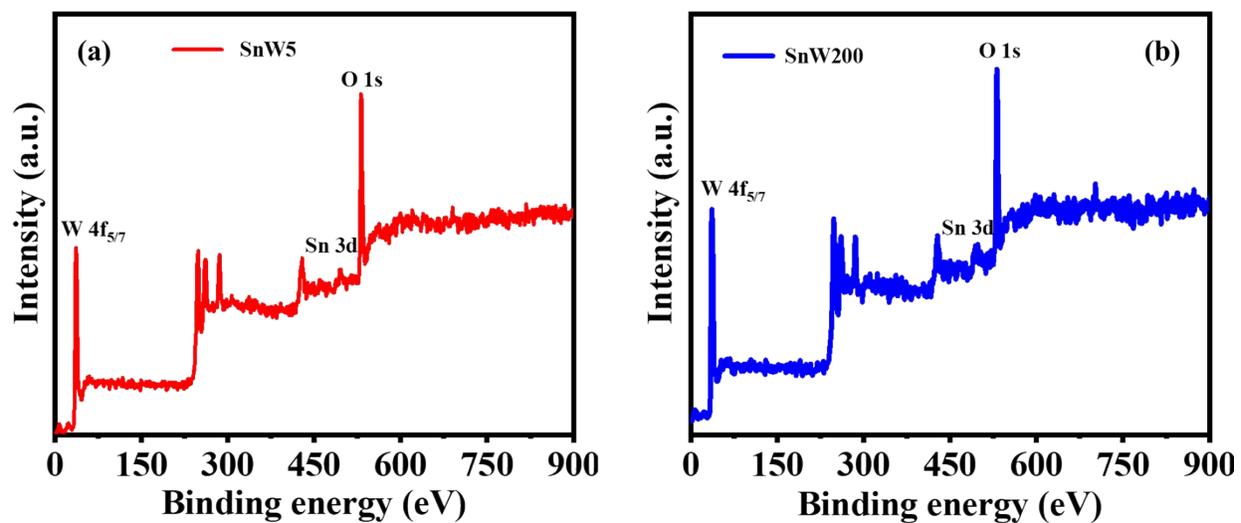Fig. S5 (a-d) Bar graph of SnW5, SnW200, SnW400, and SnW600 respectively.

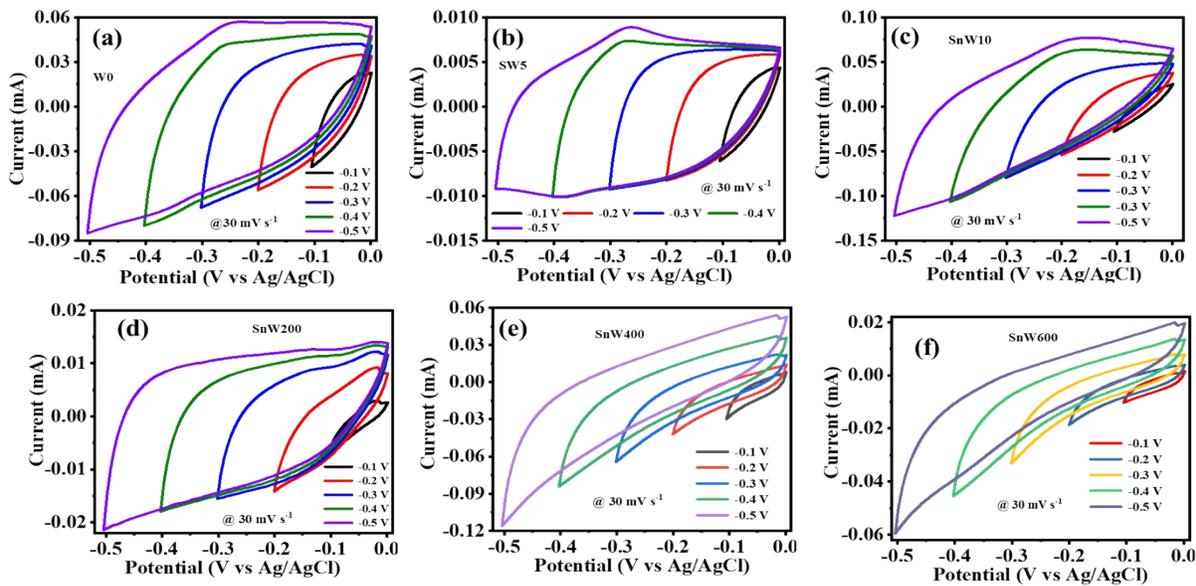Fig. S6 XPS survey scan of SnW5 (a) and SnW200 (b).

Fig. S7 (a-c) CV curves at different voltages of W0, SnW5, SnW10, (d-f) CV curve at various voltages of SnW200, SnW400, and SnW600 respectively.

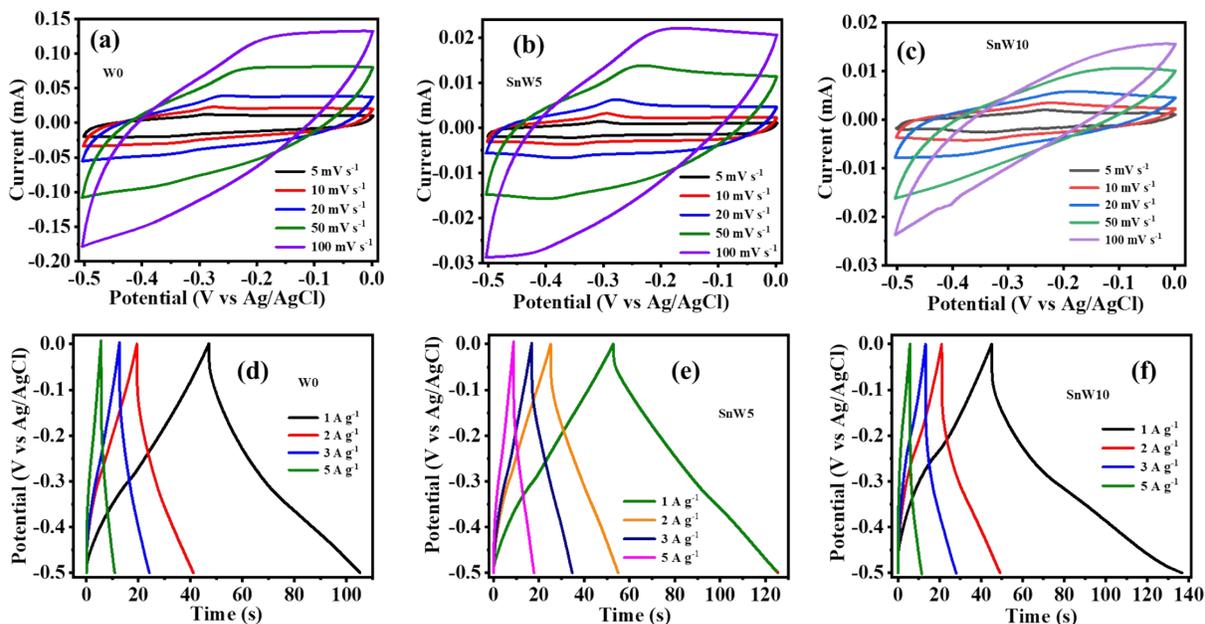Fig. S8 (a-c) CV curves at different scan rates of W0, SnW5, SnW10, (d-f) CV curve at various current densities of W0, SnW5, SnW10 respectively.
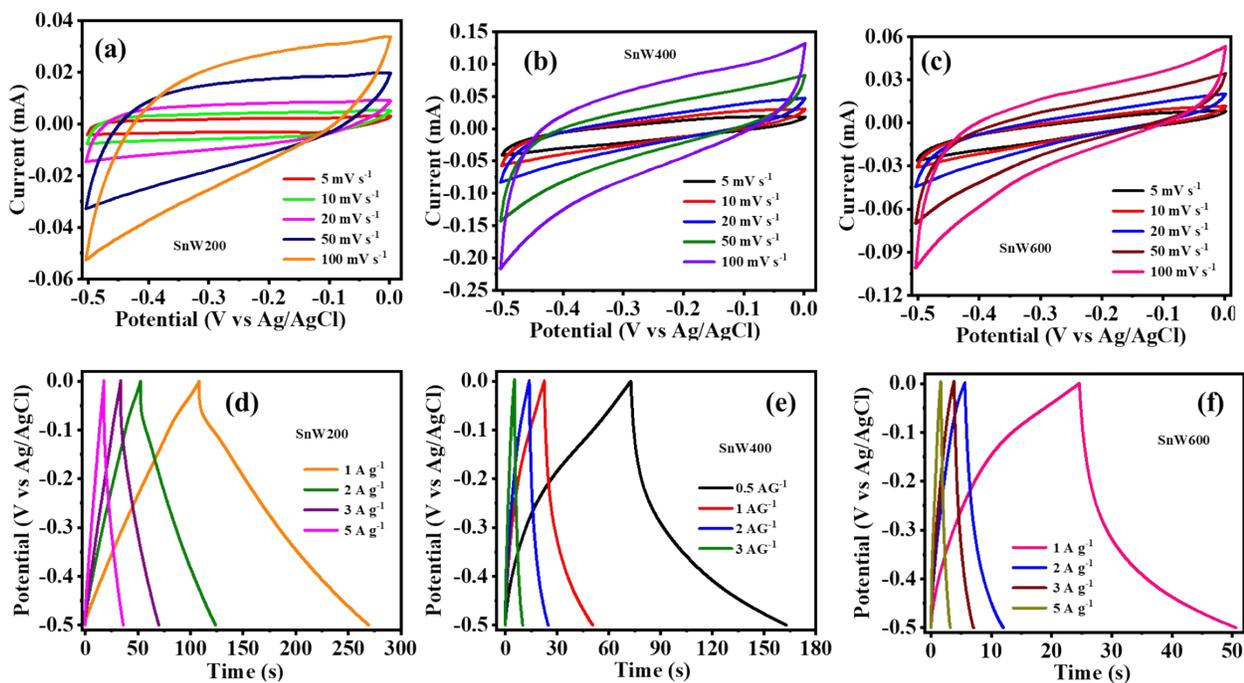
Fig. S9 (a-c) CV curves at different scan rates of SnW200, SnW400, and SnW600, (d-f) CV curve at various current densities of SnW200, SnW400, and SnW600 respectively.
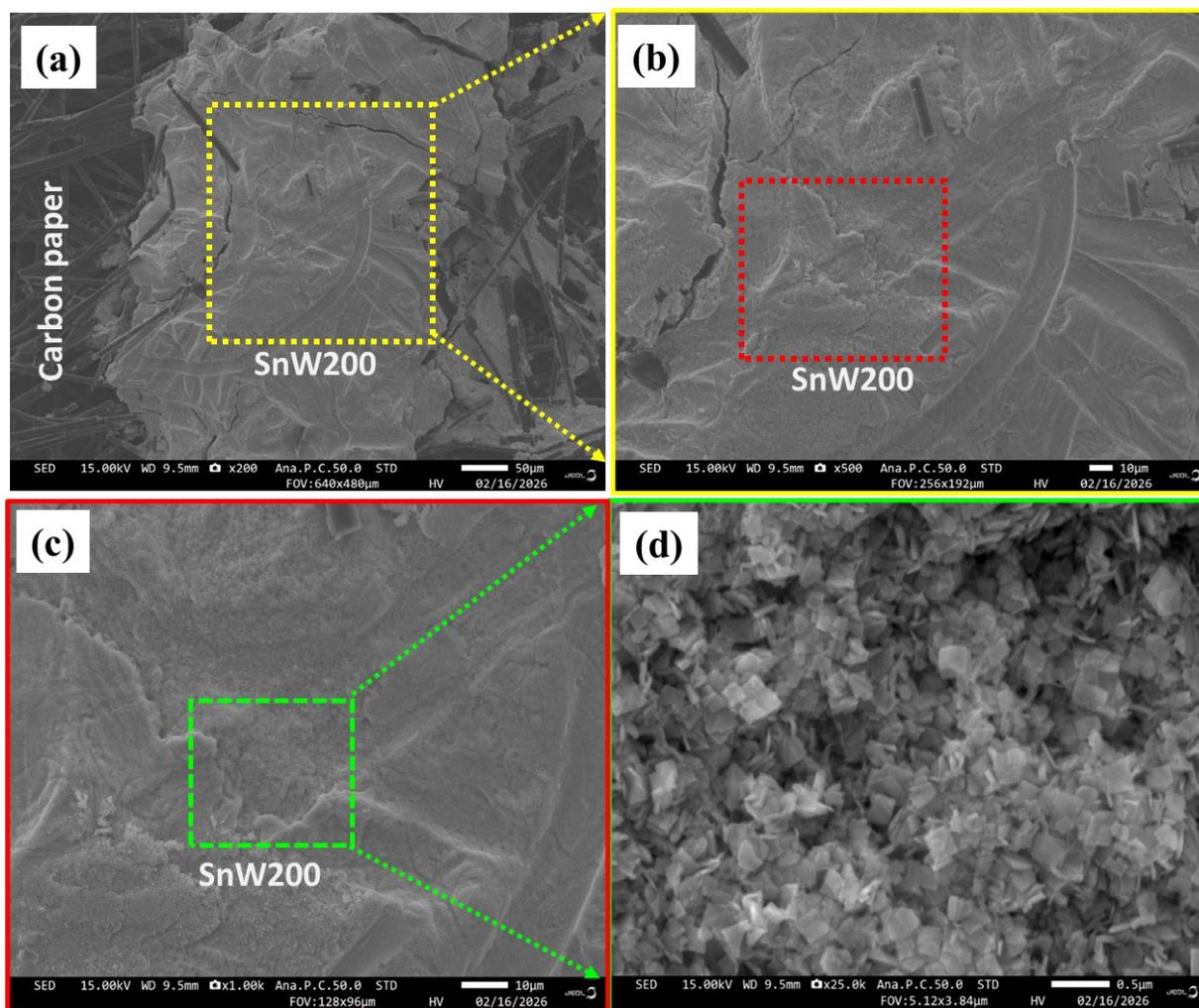
Figure S9 (a-d) SEM image of electrode (SnW200/Carbon paper) at various magnifications.
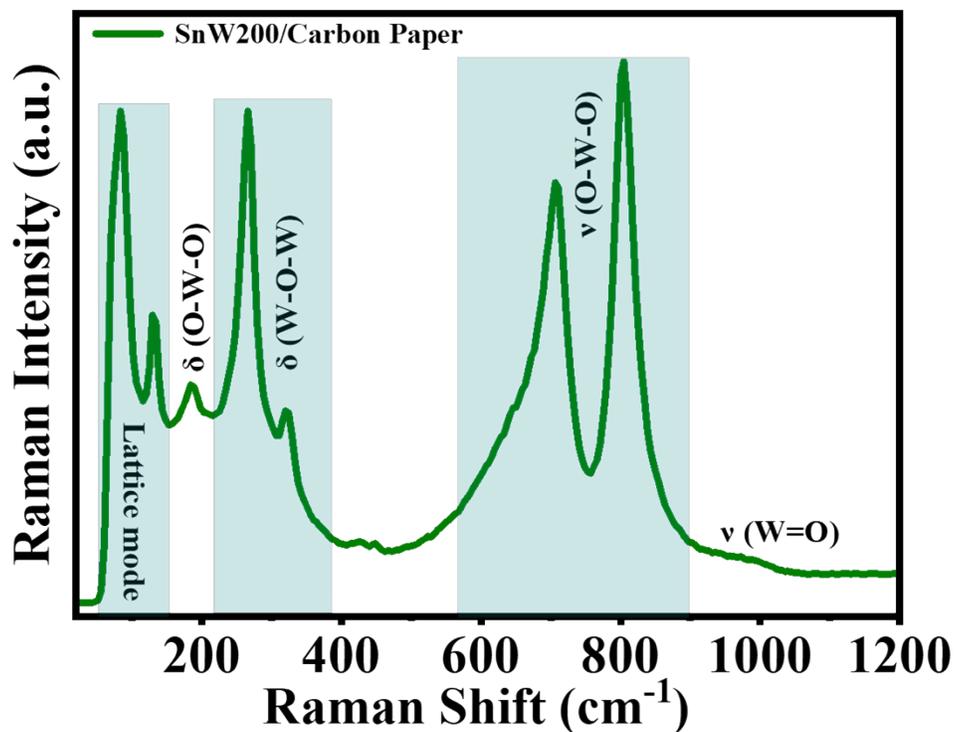
Figure S10. Raman spectra of cycled electrode (SnW200/Carbon paper).

Table S1 the electrochemical out of three electrode measurement of W0, SnW5, SnW10, SnW200, SnW400, and SnW600.

Sr. No.	Sample	Morphology	Crystal Structure	Cs (F g^{-1}) @ 1 A g^{-1}	Rs (Ω)	Rct (Ω)	Zw (Ω)
1.	W0	Nanoplate	Orthorhombic	115	1.94	64.29	66.23
2.	SnW5	Nanoplate	Orthorhombic	146	2.02	29.7	31.72
3.	SW10	Nanoplate	Orthorhombic	182	2.18	79.27	81.45
4.	SnW200	Nanoplate	Orthorhombic/Cubic	323	2.60	2.21	4.81
5.	SnW400	Nanoplate	Cubic	178	4.07	0.44	4.51
6.	SnW600	Nanoplate	Cubic	52	2.72	58.42	61.14

Table S2 Comparison table of supercapacitor performance of various WO_3 combinations with present work.

Sr. No	Material	Electrolyte	Specific capacitance	Synthesis Methods	Structure	Morphology	Stability (%)	Ref.
1	Co-WO$_3$	2 M KOH	45 F g^{-1} at 0.25 A g^{-1}	Microwave	Monoclinic	Nanoporous morphology	_	[1]
2	Zn–WO$_3$	2 M KOH	35.70 F g^{-1} at 0.25 A g^{-1}	Microwave	Monoclinic	Sphere	_	[2]
3	Ni-WO$_3$	2 M KOH	171.28 F g^{-1} at 0.25 A g^{-1}	Microwave	Monoclinic	Nanopowder	_	[3]
4	Pd-WO$_3$	1 M Na$_2$SO$_4$	33 F g^{-1} at 0.5 A g^{-1}	Hydrothermal	Monoclinic	Nanobricks assembled cauliflower	86.95 @ 1100 cycles	[4]
5	Sn-WO$_3$	1 M KOH	419 F g^{-1} at 1 A g^{-1}	Microwave	Monoclinic	_	_	[5]
6	P-WO$_3$	LiClO$_4$	120.6 F g^{-1} at 2 A g^{-1}	Hydrothermal	Monoclinic	Quantum dots	87.3 @ 4,000 cycles	[6]
7	Bi- WO$_3$	0.5 mol L^{-1} H$_2$SO$_4$	_	Sol–gel	Monoclinic	Nanosheet structure	91 @ 5040 cycles	[7]
8	Mo-WO$_3$	1 M LiClO$_4$	334.6 mF g^{-1}	Electrodeposition	_	Granules	_	[8]
9	P-WO$_3$	1 mol L^{-1} LiClO$_4$ + PC	_	Wet chemical	_	Nanograins	65.3 @ 1000 cycles	[9]
10	Nb-WO$_3$	0.5 M LiClO$_4$	_	Sol–gel	Orthorhombic	Porous structure	78.1 @ 8000 cycles	[10]
11	Ti-WO$_3$	1 M LiClO$_4$	_	Spin-coated	_	Sandwich	96.5 @ 1000 cycles	[11]
12	Gd-WO$_3$	1 M LiClO$_4$ + PC	4.25 F g^{-1} at 2 A g^{-1}	Wet-chemical	_	Nano-stalagmites	87.4 @ 2000 cycles	[12]
13	Nd−NbCo -doped SnO$_2$/α-WO$_3$	1 M LiClO$_4$ +PC	_	Dip coating	Hexagonal	Core shell	65 @ 900 cycles	[13]
14	Co-doped WO$_3$	1M H$_2$SO$_4$	_	Sol–gel spin-coating	Octahedral	Nanosheet	86.4 @ 10200 cycles	[14]
15	Nb$_2$O$_5$/ WO$_3$	1 M LiClO$_4$ + PC	_	Hydrothermal	Orthorhombic	Nanogranular flakes	98.6 @ 150 cycles	[15]
16	WO$_3$/ MXene	1 M H$_2$SO$_4$	290 F g^{-1} at 0.5 A g^{-1}	Wet chemical	Orthorhombic/ hexagonal	_	91.1@ 10,000	[16]

							cycle	
17	WO$_3$-ZnS	1 M H$_2$SO$_4$	243 F g^{-1} at 2 A g^{-1}	Microwave-assisted wet chemical method	Monoclinic	Small rod shape	100 @ 4000 cycles	[17]
18	Mn$_3$O$_4$-WO$_3$	0.5 M Na$_2$SO$_4$	101 F g^{-1} at 1 A g^{-1}	Solvothermal	_	Porous	_	[18]
19	**Sn-doped WO$_3$.H$_2$O (SnW5)**	**1 M H$_2$SO$_4$**	**146 F g^{-1} at 1 A g^{-1}**	**Wet-Chemical methods**	**Orthorhombic**	**Nanoplate**	**-**	**This work**
20	**Sn-doped WO$_3$.H$_2$O, WO$_3$ (SnW200)**	**1 M H$_2$SO$_4$**	**323 g^{-1} at 1 A g^{-1}**	**Wet-Chemical methods**	**Orthorhombic + Cubic**	**Nanoplate**	**72 @ 10000 cycles**	

Table S3 the electrochemical out of two measurements of 1st cycle, 5000th cycle, and 10,000th cycles.

Sr. No.	Sample	Rs (Ω)	Rct (Ω)	Zw (Ω)
1.	1st cycle	0.061	0.059	0.12
2.	5000th cycles	0.21	0.22	0.43
3.	10,000 cycles	0.162	0.128	0.29

References

[1]   R. Dhilip Kumar, S. Karuppuchamy, Microwave mediated synthesis of nanostructured Co -WO3 and CoWO4 for supercapacitor applications, J. Alloys Compd. 674 (2016) 384–391. https://doi.org/10.1016/j.jallcom.2016.03.074.

[2]   R.D. Kumar, Y. Andou, S. Karuppuchamy, Microwave-assisted synthesis of Zn–WO3 and ZnWO4 for pseudocapacitor applications, J. Phys. Chem. Solids 92 (2016) 94–99. https://doi.org/10.1016/j.jpcs.2016.01.022.

[3]   R.D. Kumar, Y. Andou, S. Karuppuchamy, Synthesis and characterization of nanostructured Ni-WO3 and NiWO4 for supercapacitor applications, J. Alloys Compd. 654 (2016) 349–356. https://doi.org/10.1016/j.jallcom.2015.09.106.

[4]   S.P. Gupta, V.B. Patil, N.L. Tarwal, S.D. Bhame, S.W. Gosavi, I.S. Mulla, D.J. Late, S.S. Suryavanshi, P.S. Walke, Enhanced energy density and stability of self-assembled cauliflower of Pd doped monoclinic WO3 nanostructure supercapacitor, Mater. Chem. Phys. 225 (2019) 192–199. https://doi.org/10.1016/j.matchemphys.2018.12.077.

[5]   N. Dharmalingam, S. Rajagopal, P. Veluswamy, S. Paulraj, V. Kathirvel, Facile microwave synthesis of Sn-doped WO3 for pseudocapacitor applications, J. Mater. Sci. Mater. Electron. 33 (2022) 9246–9255. https://doi.org/10.1007/s10854-021-07249-8.

[6]   M.-H. Jo, K.-H. Kim, H.-J. Ahn, P-doped carbon quantum dot graft-functionalized amorphous WO3 for stable and flexible electrochromic energy-storage devices, Chem. Eng. J. 445 (2022) 136826. https://doi.org/10.1016/j.cej.2022.136826.

[7]   Q. Sun, S. Li, X. Yu, Y. Zhang, T. Liu, J.Y. Zheng, Amorphous bismuth-doped WO3 film: Fast-switching time and high-performance proton-based aqueous electrochromic device, Appl. Surf. Sci. 641 (2023) 158510. https://doi.org/10.1016/j.apsusc.2023.158510.

[8]   S. Xie, Z. Bi, Y. Chen, X. He, X. Guo, X. Gao, X. Li, Electrodeposited Mo-doped WO3 film with large optical modulation and high areal capacitance toward electrochromic energy-storage applications, Appl. Surf. Sci. 459 (2018) 774–781. https://doi.org/10.1016/j.apsusc.2018.08.045.

[9]   H. Gu, M. Tan, T. Wang, J. Sun, J. Du, R. Ma, W. Wang, D. Hu, Boosting the electrochromic performance of P-doped WO 3 films via electrodeposition for smart window applications, RSC Adv. 14 (2024) 10298–10303. https://doi.org/10.1039/D4RA00979G.

[10]   C. Wu, Z. Shao, W. Zhai, X. Zhang, C. Zhang, C. Zhu, Y. Yu, W. Liu, Niobium Tungsten Oxides for Electrochromic Devices with Long-Term Stability, ACS Nano 16 (2022) 2621–2628. https://doi.org/10.1021/acsnano.1c09234.

[11]   Q. Meng, S. Cao, J. Guo, Q. Wang, K. Wang, T. Yang, R. Zeng, J. Zhao, B. Zou, Sol-gel-based porous Ti-doped tungsten oxide films for high-performance dual-band electrochromic smart windows, J. Energy Chem. 77 (2023) 137–143. https://doi.org/10.1016/j.jechem.2022.10.047.

[12]   Y. Yin, Y. Zhu, P. Liao, X. Yuan, J. Jia, C. Lan, C. Li, Co-sputtering construction of Gd-doped WO3 nano-stalagmites film for bi-funcional electrochromic and energy storage applications, Chem. Eng. J. 487 (2024) 150615. https://doi.org/10.1016/j.cej.2024.150615.

[13]   R. Goei, A.J. Ong, J.H. Tan, J.Y. Loke, S.K. Lua, D. Mandler, S. Magdassi, A.I. Yoong Tok, Nd–Nb Co-doped SnO 2 /α-WO 3 Electrochromic Materials: Enhanced Stability and Switching Properties, ACS Omega 6 (2021) 26251–26261. https://doi.org/10.1021/acsomega.1c03260.

[14]   J.Y. Zheng, Q. Sun, H. Yang, S. Yu, M. Li, X. Yu, C. Wang, T. Liu, S. Li, Amorphous bismuth and GO co-doped WO 3 electrochromic film with fast-switching time and long-term stability, Dalt. Trans. 53 (2024) 2460–2464. https://doi.org/10.1039/D3DT03805J.

[15]   P.J. Morankar, R.U. Amate, A.M. Teli, S.A. Beknalkar, C.-W. Jeon, Exploring electrochromic performance via layered deposition of tungsten oxide on niobium oxide composite electrode, J. Power Sources 613 (2024) 234930. https://doi.org/10.1016/j.jpowsour.2024.234930.

[16]   H.S. Nishad, S.M. Mane, S.P. Patole, J. Lee, S. Gosavi, P.S. Walke, Temperature driven pseudocapactive performance of WO3/MXene nanocomposite for asymmetric aqueous supercapacitors, Chem. Eng. J. 495 (2024) 153360. https://doi.org/10.1016/j.cej.2024.153360.

[17]   P. Palanisamy, K. Thangavel, S. Murugesan, S. Marappan, M. Chavali, P.F. Siril, D.V. Perumal, Investigating the synergistic effect of hybridized WO3-ZnS nanocomposite prepared by microwave-assisted wet chemical method for supercapacitor application, J. Electroanal. Chem. 833 (2019) 93–104. https://doi.org/10.1016/j.jelechem.2018.11.026.

[18]   S. Rudra, J. K, G. Thamizharasan, M. Pradhan, B. Rani, N.K. Sahu, A.K. Nayak, Fabrication of Mn3O4-WO3 nanoparticles based nanocomposites symmetric supercapacitor device for enhanced energy storage performance under neutral electrolyte, Electrochim. Acta 406 (2022) 139870. https://doi.org/10.1016/j.electacta.2022.139870.